Journal of ELECTRONIC MATERIALS, Vol. 45, No. 11, 2016
DOI: 10.1007/s11664-016-4798-5

Growth, Optical, Dielectric and Ferroelectric Properties of Non-Linear Optical Single Crystal: Glycine-Phthalic Acid

SAGADEVAN SURESH[1,2]

1.—Department of Physics, AMET University, Kanathur, Chennai 603112, India. 2.—e-mail: drsureshphysics@gmail.com

Single crystals of glycine-phthalic acid (GPA) were grown by slow evaporation process using aqueous solution. X-ray diffraction analysis was used to examine its cell structure and it was found that the GPA crystal corresponded to the orthorhombic system. To identify absorption range and cut-off wavelength for the GPA crystal, UV-visible spectrum was recorded. UV-visible spectroscopy was used to study the optical constants such as the refractive index, the extinction coefficient, electrical susceptibility, and optical conductivity. As a function of different frequencies and temperatures, the dielectric constant and the dielectric loss were examined. The electrical properties like plasma energy, Penn gap, Fermi energy, and polarizability were determined for the analysis of the second harmonic generation (SHG). Using the Kurtz powder technique, the SHG of the GPA crystal was studied. Investigations relating to hysteresis were carried out to ascertain the ferroelectric nature of the material.

Key words: Solution growth technique, NLO, SHG, XRD, UV-Visible spectroscopy, ferroelectric material

INTRODUCTION

The possibility of wide applications of non-linear optical (NLO) materials in the fast-growing and interesting fields of photonics, fiber optic communications, frequency doubling, and optical signal processing is attracting the attention of researchers.[1,2] For the development of laser systems, the key step is the efficient optical frequency conversion of NLO crystals. These systems are extremely important as broad range tuneable sources of coherent illumination in the ultraviolet, visible and near-infrared spectral regions. The present work aims to design a new material that can be considered as a second-order optical method and can have strong interaction with the oscillating electric field of light.[3] Active research is much required to produce optical devices for specific efficiencies or devices with improved performance, and it can be accomplished by the selection of suitable organic non-linear optical materials.[4,5] The amino acids are known as the finest organic materials which play a vital role in the field of non-linear optical crystal growth. The natural amino acids contain a donor NH_2 and an acceptor COOH and hence exhibit individual non-linear optical properties.[6] The fact that amino acids play an important role in the field of non-linear optical crystal growth cannot be gainsaid. The non-linear optical effect has been observed from a great number of individual natural amino acids. For the optical second harmonic generation (SHG), a greater promise is found in the complex of amino acids. Presently, the demand is for not compromising on the quality and size of the crystals but to achieve the rapid growth in a shorter period of time. The deviation of physical, optical, and electrical properties of these materials is important for the development of novel NLO materials and is achieved by adding functional groups or by including dopants for different/modified applications. Dopants analysis is useful in the enhancement of growth-promoting factors such as growth rate and other convenient physical properties like optical transparency, SHG efficiency, laser damage threshold (LDT), etc.

(Received December 20, 2015; accepted July 8, 2016; published online July 28, 2016)

Ferroelectric crystals have been grown by distinct groups and considerable analysis has been accomplished. Many researchers have made a lot of efforts to grow ferroelectric crystals by examining the mechanism of ferroelectric phase transition.[7–10] Although it has been stated by many that glycine is incorporated into inorganic materials to form single crystals, only a few of such crystals have been reported to have both ferroelectric and non-linear properties. Hence, this paper has focuses on the growth aspects being developed by SHG slow evaporation method of the organic GPA crystals. The single crystal XRD examination has established lattice parameters. UV-Visible examination has helped to determine the absorption range for the given material. The SHG of the GPA crystal was examined by the Kurtz powder method. Studies were made of the dielectric constant and the dielectric loss for different temperatures and frequencies.

EXPERIMENTAL

Analytical reagent grade chemicals of glycine (Merck; 99%) and phthalic acid (Merck; 98%) supplied by Merck (India) were employed without further purification. GPA was grown from 7.5 g glycine ($C_2H_5NO_2$) and 16.61 g phthalic acid ($C_6H_4(COOH)_2$ taken in equimolar ratio (1:1). The calculated amounts of the reactants were thoroughly dissolved in triple-distilled water and stirred well for about 6 h. Then, the solution was filtered and transferred to a crystal growth vessel and crystallization was allowed to take place by the slow evaporation technique at room temperature. The saturated solution was further purified and then allowed to evaporate at a higher temperature. The synthesized material was purified by repeatedly recrystallizing it. The formation of tiny seed crystals with good transparency was due to the spontaneous nucleation. From these crystals, a flawless seed crystal was selected and suspended in the mother solution so as to enable it to evaporate at room temperature. Due to the formation of monomers at the seed crystal sites, single crystals with large size were obtained from the mother solution, after the completion of the nucleation and growth processes. The solvent was allowed to evaporate slowly and in a growth period of 24 days, and a GPA crystal of dimensions of about $10 \times 8 \times 6$ mm^3 was obtained. The photograph of the grown GPA crystal is shown in Fig. 1.

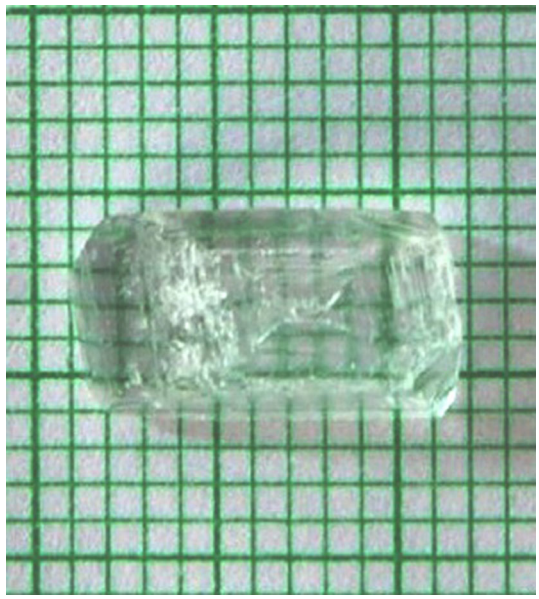

Fig. 1. GPA crystal.

RESULTS AND DISCUSSION

Single-Crystal X-ray Diffraction

An ENRAF-NONIUS CAD 4 automatic x-ray diffractometer was used for the analysis of single crystal x-ray diffraction and for the determination of the lattice parameters. The results of the XRD analysis revealed that the grown crystal had an orthorhombic structure with a Pbca space group and the lattice parameter values of the grown crystal were a = 7.654 Å, b = 21.062 Å, and c = 11.275 Å. The single crystal data were found to agree well with the reported values.[11]

UV-NIR-VIS-Spectral Analysis

Figure 2 exhibits a VARIAN CARY MODEL 5000 spectrophotometer spectrum in the wavelength range of 200–800 nm, which was used in this study for producing the optical absorption spectrum of the GPA single crystal. The optical absorption analysis plays a significant role in identifying the benefit of an NLO material both in the visible and the blue regions. Information about the structure of the molecules was provided by UV-vis spectral analysis and the absorption of the UV and visible light engages in the promotion from the ground state to the higher energy state electron in the σ and π orbitals. In the considered region of wavelength, optical fabrications require the crystal to be highly transparent.[12,13] In the entire visible region, the favorable transmittance of the crystal indicates its suitability for SHG.[14] It was noticed that the UV absorption edge for the grown crystal was nearly 285 nm. The band structure and the type of transition of the electrons studied were based on the fact that the optical absorption coefficient depends on photon energy.[15–17] The optical absorption coefficient (α) was computed from the transmittance using the following relationship:

$$\alpha = \frac{1}{d} Ln\left(\frac{1}{T}\right) \quad (1)$$

where T is the transmittance and d is the thickness of the crystal. Being a direct band gap material, the

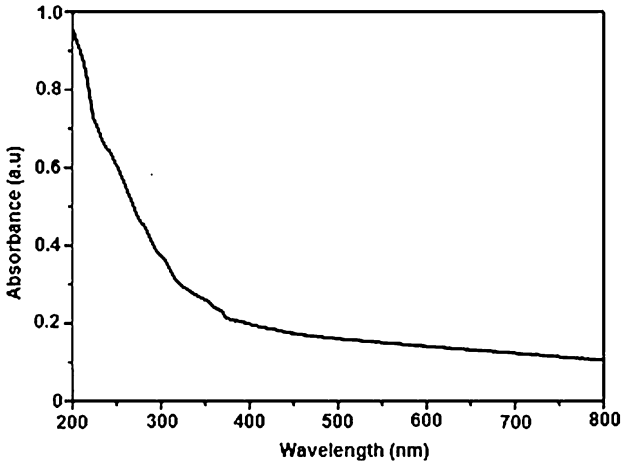

Fig. 2. UV-Visible absorption spectrum of GPA crystal.

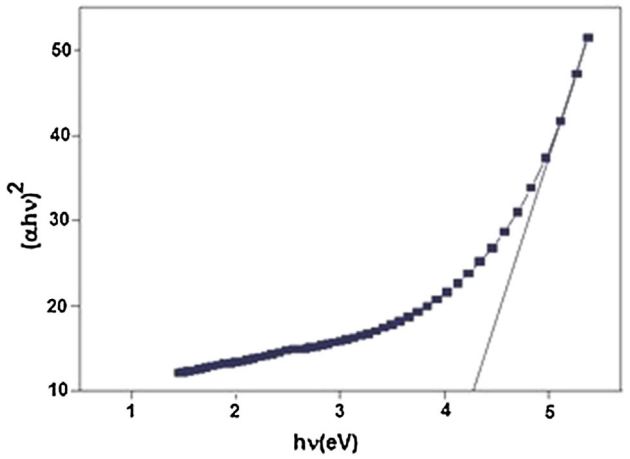

Fig. 3. Plot of $(\alpha h\nu)^2$ versus $(h\nu)$.

crystal under study has an absorption coefficient (α) obeying the following relationship for high photon energies ($h\nu$):

$$\alpha = \frac{A(h\nu - E_g)^{1/2}}{h\nu} \tag{2}$$

where E_g is the optical band gap of the crystal and A is a constant. A plot of $(\alpha h\nu)^2$ versus $h\nu$ is shown in Fig. 3. E_g could be evaluated using the extrapolation of the linear part. The bandgap was found to be 4.35 eV and the large band gap clearly indicated the wide transparency of the crystal. The lower cut-off wavelength could be computed from the absorption spectrum and was found to be 285 nm. The crystal did not resist the transmission of the laser beam which was indicated by the lower percentage absorption in the range between 285 nm and 800 nm. This information in turn indicated that the grown crystal had a good transparency in the UV-visible and near-IR region and it could be inferred that the crystal would meet the requirements for use in NLO applications. The internal efficiency of the device depends upon the absorption coefficient, which is the reason for the tailoring of the absorption coefficient and the tuning of the band gap of the material that can help produce the desired material, which becomes suitable for fabricating various layers of the optoelectronic devices as per the user's requirements.[18]

Determination of Optical Constants

The extinction coefficient (K) can be achieved from the following equation:

$$K = \frac{\lambda\alpha}{4\pi} \tag{3}$$

The extinction coefficient (K) was found to be 0.000546 at λ = 800 nm. The transmittance (T) is given by:

$$T = \frac{(1-R)^2\exp(-\alpha t)}{1 - R^2\exp(-2\alpha t)} \tag{4}$$

Reflectance (R) in terms of absorption coefficient could be obtained from the above equation. Hence, we have:

$$R = \frac{1 \pm \sqrt{1 - \exp(-\alpha t + \exp(\alpha t)}}{1 + \exp(-\alpha t)} \tag{5}$$

The refractive index *(n)* cab be determined from the reflectance data using the following equation:

$$n = -\frac{(R+1) \pm \sqrt{3R^2 + 10R - 3}}{2(R-1)} \tag{6}$$

The refractive index (n) was found to be 1.78 at λ = 800 nm. The high refractive index makes the GPA crystal suitable for use in optoelectronic devices. From the optical constants, electric susceptibility (χ_c) can be calculated from the following relationship:

$$\varepsilon_r = \varepsilon_0 + 4\pi\chi_C = n^2 - k^2 \tag{7}$$

whence

$$\chi_C = \frac{n^2 - k^2 - \varepsilon_0}{4\pi} \tag{8}$$

where ε_0 is the permittivity of free space. The value of electric susceptibility χ_C was found to be 2.168 at λ = 800 nm. The optical behavior and the dielectric behavior of the crystal ccanould be correlated. The complex dielectric constant is one of the most fundamental intrinsic material properties, the real part of which broadly directs how much it will slow down the speed of light in the material, while its imaginary part describes how a dielectric absorbs energy from the electric field due to dipole motion.[19] The real part dielectric constant ε_r and the imaginary part dielectric constant ε_i can be calculated from the following relationships

$$\varepsilon_r = n^2 - k^2$$

$$\varepsilon_i = 2nk \tag{9}$$

The values of the real (ε_r) and the imaginary (ε_i) dielectric constants at λ = 800 nm were estimated to be 2.874 and 5.635 × 10^{-5}, respectively. For NLO application, the optical band gap suggests that the material has the required transmission range and moderate values of the refractive index. As one of the powerful tools, optical conductivity is used for studying the electronic states in materials. The optical conductivity (σ) of the crystal was calculated using the following relationships:

$$\sigma = \frac{\omega}{4\pi}\mathrm{Im}(\varepsilon) \tag{10}$$

where the value of Im (ε) is given by:

$$\mathrm{Im}(\varepsilon) = \frac{C^2}{\omega^2(\mu_r)}(k\alpha) \tag{11}$$

where μ_r is the relative permeability. For most crystalline materials μ_r is very close to 1 at optical frequencies. On putting the value of Im (ε) in Eq. 10, we get:

$$\sigma = \frac{\alpha nc}{4\pi} \tag{12}$$

where c is the velocity of light, α is the absorption coefficient, and n is the refractive index. When the material was irradiated with light, the optical conductivity as a function of the frequency response was calculated by using the following relationship and its value was found to be 1.62 × 10^7 s^{-1} at 800 nm. The electrical conductivity can also be estimated by the optical method using the following relationship:

$$\sigma_e = \frac{2\lambda\sigma}{\alpha} \tag{13}$$

The electrical conductivity was found to be 2.85 × 10^{10} O^{-1} cm^{-1} at 800 nm. The material could allow all radiations to pass through it in the wavelength range of 280–800 nm. This can be counted as an advantage because there is no change in the transmittance in the entire visible region which is imperative for materials having NLO properties.

Refractive Index Measurements

Measurements of the refractive index required the use of well-polished crystals of the as-grown GPA. Brewster's angle (θp) for the GPA was measured and was found to be 60.52°. The refractive index was computed using the equation n = tanθp, where θp is the polarizing angle which measured 1.76. The refractive index was obtained as 1.76 which was very close to that (1.78) obtained from using UV-vis spectroscopy.

Dielectric Studies

The dielectric studies of the grown crystal were carried out by using a HIOCKI 3532-50 LCR HITESTER. A crystal of dimension 1 × 0.5 × 0.1 cm^3 having a silver coating on the opposite faces was placed between the two copper electrodes and a parallel plate capacitor was thus formed. The measurements were made at frequencies ranging from 50 Hz to 5 MHz at different temperatures. The dielectric constant (ε_r) and the dielectric loss were calculated using Eqs. 14 and 15:

$$\varepsilon_r = \frac{Cd}{\varepsilon_0 A} \tag{14}$$

$$\varepsilon_i = \varepsilon_r \tan\delta \tag{15}$$

$$\tan\delta = \frac{\varepsilon_i}{\varepsilon_r} \tag{16}$$

where d is the thickness of the crystal, A is the area of the crystal, C is the capacitance and ε_0 is the permittivity of free space. Figure 4 shows the plot of the dielectric constant versus log frequency, from which It can be seen that the dielectric constant decreases as the frequency increases and acquires high values at low frequencies. This could be ascribed to the loosely bonded ions in the lower frequency region in the crystal. It was at the crystal surface that the predominance of conductance due to the trading of electrical charges in the low frequency region could be detected, which led to the local displacement of electrons in the direction of the applied field. The frequency impacts the dipoles in such a manner that the dipoles do not comply with the varying external field and consequently decrease the value of the dielectric constant in the low frequency region.[20] Likewise, the dependence of the dielectric loss on frequency is shown in Fig. 5. The dielectric loss was realised to be high at low frequency and was decreasing in the higher frequency region. That the were fewer defects was indicated by the low value of the dielectric loss at high frequency, and the sample had superior optical quality where this parameter is of vital importance for NLO materials.[21] From Figs. 4 and 5, it is also observed that the dielectric constant and the dielectric loss increase with an increase in temperature, which is attributed to the presence of space charge polarization near the grain boundary interfaces, which depends on the purity and perfection of the crystal. For the making of microelectronic and nonlinear optical devices, this behavior proves advantageous. The electrical properties are very necessary to analyze the SHG efficiency of the GPA crystal. The valence electron plasma energy, $\hbar\omega_p$, is evaluated using the relationship:

$$\hbar\omega_P = 28.8\left(\frac{Z\rho}{M}\right)^{1/2} \tag{17}$$

According to the Penn model, the average energy gap for GPA is given by:

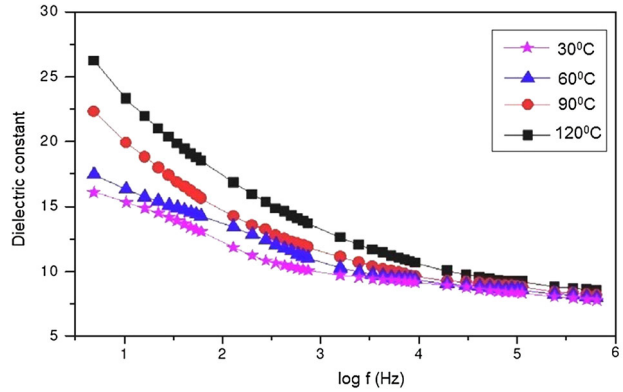

Fig. 4. Variation of dielectric constant with log frequency.

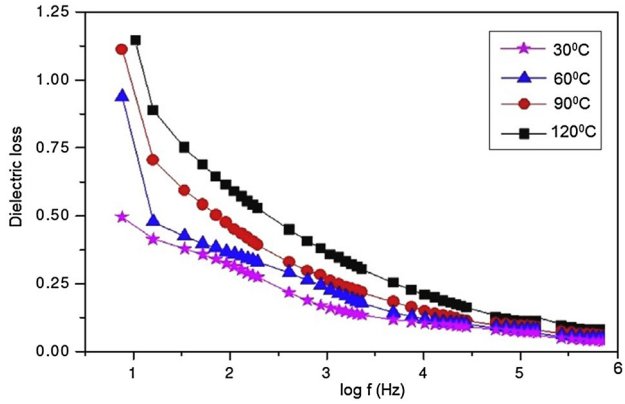

Fig. 5. Variation of dielectric loss with log frequency.

$$E_P = \frac{\hbar\omega_P}{(\varepsilon_\infty - 1)^{1/2}} \tag{18}$$

where $\hbar\omega_p$ is the valence electron Plasmon energy and the Fermi energy given by:

$$E_F = 0.2948(\hbar\omega_P)^{4/3} \tag{19}$$

Then, we obtain electronic polarizability (α) using the relationship:

$$\alpha = \left[\frac{(\hbar\omega_P)^2 S_0}{(\hbar\omega_P)^2 S_0 + 3E_P^2}\right] \times \frac{M}{\rho} \times 0.396 \times 10^{-24} cm^3 \tag{20}$$

where S_0 is a constant given by:

$$S_0 = 1 - \left[\frac{E_P}{4E_F}\right] + \frac{1}{3}\left[\frac{E_P}{4E_F}\right]^2 \tag{21}$$

The value of α obtained from Eq. 20 closely matches with that obtained using Clausius-Mossotti relationship:

$$\alpha = \frac{3}{4}\frac{M}{\pi N_a \rho}\left[\frac{\varepsilon_\infty - 1}{\varepsilon_\infty + 2}\right] \tag{22}$$

Considering that the polarizability is highly sensitive to the bandgap, the following empirical relationship is also used to calculate:

$$\alpha = \left[1 - \frac{\sqrt{E_g}}{4.06}\right] \times \frac{M}{\rho} \times 0.396 \times 10^{-24} cm^3 \tag{23}$$

where E_g is the bandgap value determined through the UV absorption spectrum. For calculating the physical or electronic properties of materials, the very important parameter is the high-frequency dielectric constant of materials. These values of GPA are compared with those of the standard material KDP and listed in Table I, from which it can be noted that the electrical properties are higher than those of KDP. In particular, the polarizability was found to be 0.6 times higher for GPA than for KDP.[22]

NLO Test: Kurtz Powder SHG Method

The crystal was densely packed in a microcapillary tube of uniform bore and before that it was powdered. A Q-switched Nd:YAG laser beam of wavelength 1064 nm with an input power of 6.2 mJ/pulse and a pulse width of 8 ns with a repetition rate of 10 Hz was made to fall orthogonally on the sample. The output from the sample was monochromated to gather the intensity of the 532 nm component and to exclude the fundamental wavelength. The green radiation signal voltage (6 mV) was measured with the appropriate system which was observed from the sample. The SHG efficiency of the GPA crystal was compared with the KDP reference (10 mV) , and it was found that the SHG efficiency of GPA was 0.6 times that of the KDP reference crystal. It could be observed that the conversion efficiency of GPA was 0.6 times more than that of the KDP crystal.

Ferroelectric Studies

The fact that an electric field can cause a reversal of polarization (switching) in ferroelectric materials contributes to the most significant characteristic of such materials. A multi-domain state is that of a ferroelectric material to scale back (in ceramics) or utterly take away (in crystals) the domain walls to which an electrical field is to be applied. The occurrence of the ferroelectric hysteresis loop is caused by the domain-wall switching in ferroelectric materials.[23] A ferroelectric loop tracer (Radiant Technologies) determines the ferroelectric property of the crystal. Figure 6 exhibits the plot of polarization versus voltage behavior where the voltage ranges from +200 to −200 V of the grown crystal. It can be studied from the figure that the material has good ferroelectric characteristics with the measured (Pr) remanent polarization and (Vr) coercive voltage values being 28 nC/cm^2 and 180 V, respectively.[24,25] The saturation of the loops indicates that the losses are minimal at these low frequencies, so it is suggested that the crystal with electrical resistivity ρ = 6.3 × 10^6 Ω cm^2 is highly resistive.

Table I. Electronic properties of the GPA and KDP single crystals

Parameter	GPA crystal	KDP crystal
Plasma energy ($\hbar\omega_p$)	17.88 eV	17.28 eV
Penn gap (E_P)	2.97 eV	2.37 eV
Fermi Energy (E_F)	12.62 eV	12.02 eV
Electronic polarizability (using Penn analysis)	2.27×10^{-23} cm^3	2.12×10^{-23} cm^3
Electronic polarizability (using Clausius–Mosotti equation)	2.28×10^{-23} cm^3	2.14×10^{-23} cm^3
Electronic polarizability (using bandgap)	2.26×10^{-23} cm^3	2.10×10^{-23} cm^3

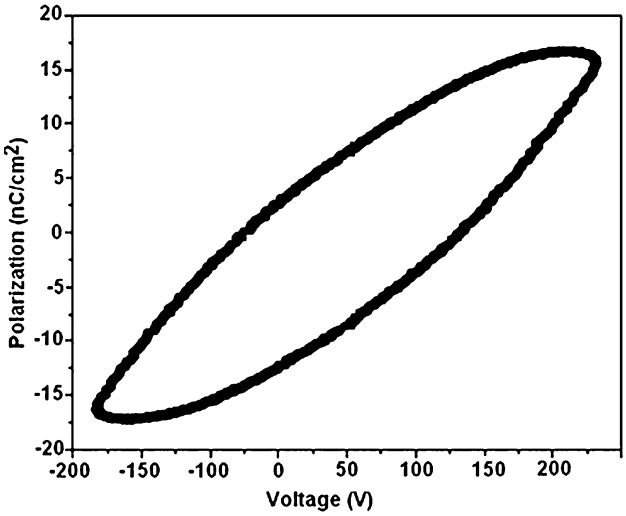

Fig. 6. Hysteresis studies of the GPA crystal.

CONCLUSIONS

The slow evaporation technique was used to grow a single crystal of GPA. Single crystal XRD synthesis confirmed that the crystal was associated with the orthorhombic system. The excellent transmission in the entire visible region was ascertained by a UV-visible absorption spectrum. The optical properties such as the band gap, refractive index, reflectance, extinction coefficient and electrical susceptibility were studied. By using the Brewster's angle technique, the refractive index was determined. At different temperatures, the dielectric constant and the dielectric loss were examined as a function of frequency. The computation of electrical properties such as plasma energy, Penn gap, Fermi energy and polarizability was carried out. The SHG efficiency was more than that of the standard material, KDP, whichwas indicated by the higher value of polarizability. With the help of the Kurtz and Perry powder method, the theoretical prediction of SHG efficiency was confirmed. From the powerful field and spontaneous polarization, values were computed from the physical phenomenon examination. GPA was thus found to be a most efficient NLO material with an acceptable SHG effectiveness that is needed for significant applications in the field of optoelectronics and photonics. Due to better optical and dielectric properties, this material was found to exhibit NLO behavior remarkably.

REFERENCES

1. D.R. Askeland and P.P. Phule, *The Science and Engineering of Materials* (London: Thomson, 2003).
2. C.A. Gonsago, H.M. Albert, P. Malliga, and A.J.A. Pragasam, *Mater. Manuf. Process.* 27, 355 (2012).
3. R.A. Kumar, R. Ezhilvizhi, N. Vijayan, and D.R. Babu, *Phys. B* 406, 2594 (2011).
4. T. Kishore Kumar, S. Pandi, M.V. Antony Raj, C.M. Magdalene, and D. Prem Anand, *Mater. Manuf. Process.* 25, 978 (2010).
5. M. Prakash, D. Geetha, and M. Lydia Caroline, *Mater. Manuf. Process.* 27, 519 (2012).
6. G.R. Dillip, G. Bhagavannarayana, P. Raghavaiah, and B. Deva Prasad Raju, *Mater. Chem. Phys.* 134, 371 (2012).
7. R. Shanmugavadivu, G. Ravi, and A. Nixon Azariah, *J.Phys. Chem. Solids.* 67, 1858 (2006).
8. M. Narayan Azariah and S.M. Dharmaprakash, *J Crystal Growth.* 235, 511 (2002).
9. C. Preethy Menona, J. Philipa, A. Deepthy, and H. L. Bhat, *Mater. Res. Bull.* 36, 2407 (2001).
10. K. Rajarajan, G.P. Joseph, S.M. Ravi Kumar, I.V. Potheher, A.J.A. Pragasam, K. Ambujam, and P. Sagayaraj, *Mater. Manuf. Process.* 22, 370 (2007).
11. T. Balakrishnan, K. Ramamurthi, and S. Thamotharan, *Acta Cryst.* E69, 057 (2013).
12. S. Suresh, *Optik Int. J. Light Electron Opt.* 125, 950 (2014).
13. S. Suresh, *Optik-Int. J. Light Electron Opt.* 125, 1223 (2014).
14. S. Suresh and D. Arivuoli, *J. Optoelectron. Biomed. Mater.* 3, 63 (2011).
15. P. Koteeswari and S. Suresh, *J. Mater.* 362678, 7 (2014).
16. S. Suresh, *Optik Int. J. Light Electron Opt.* 125, 2826 (2014).
17. V. Azeezaa, A.J.A. Pragasam, T.G. Sunitha, P. Koteeswari and S. Suresh, *Acta Phys. Polonica A.* 128, 423 (2015).
18. S. Suresh, *Optik Int. J. Light Electron Opt.* 127, 5613 (2016).
19. G. Govindasamy, P. Murugasen, and S. Suresh, *Mater. Res.* 19, 413 (2016).
20. N. Nithya, R. Mahalakshmi, and S. Suresh, *Mater. Res.* 18, 581 (2015).
21. S. Suresh, *Optik Int. J. Light Electron Opt.* 126, 317 (2015).
22. S.K. Kurtz and T.T. Perry, *J. Appl. Phys.* 39, 3798 (1968).
23. D. Damjanovic, in *Hysteresis in Piezoelectric and Ferroelectric Materials*, ed. by G. Bertotti, I. Mayergoyz. The Science of Hysteresis (Academic Press is an Imprint of Elsevier, The Boulevard, Langford lane, Kidlington, Oxford, 2006).
24. J. Shieh, J.H. Yeh, Y.C. Shu, and J.H. Yen, *Mater. Sci. Eng., B* 161, 50 (2009).
25. D. Lebeugle, D. Colson, A. Forget, M. Viret, P. Bonville, J.-F. Marucco, and S. Fusil, *Phys. Rev. B* 76, 024116 (2007).